Evaluation of the Gamma Law for Settling Velocity and Trapping Capacity Analysis of Suspended Particles in a Dam Reservoir (Lobo River in Côte d'Ivoire)

Bérenger Koffi [1,2,*], Martin Sanchez [2], Zilé Alex Kouadio [1], Michal Habel [3], Jules Sekedoua Kouadio [4], Kouamé Olivier Jean Kouadio [1], Dibi Brou [1] and Kouakou Lazare Kouassi [1]

[1] Laboratory of science and Technology of Environment, Jean Lorougnon Guédé University, Daloa BP 150, Côte d'Ivoire
[2] UMR 6112 CNRS, LPG (Lab. Planetologie et de Géosciences), Nantes University, 2 rue de la Houssinière, BP 92208, CEDEX 3, 44322 Nantes, France
[3] Facullty of Geographical Sciencesy, Kazimierz Wielki University, 85-033 Bydgoszcz, Poland
[4] Laboratoire Eau et Environnement (LEE), Université Gustave Eiffel, Allée des Ponts et Chaussées, CS 5004, 44344 Bouguenais, France
[*] Correspondence: berenger.koffi@univ-nantes.fr

Abstract: Human activities and climate change are currently dominant processes that affect hydrological processes, resulting in alterations in water and sediment flows. Evaluation of the settling velocity of suspended solids is a critical parameter in modelling sediment transport. In this study, we investigated seasonal changes in suspended solids' settling velocity and trapping capacity in the presence and absence of water turbulence on a dam reservoir. Using key parameters such as flow rate, mean settling velocity ($\overline{V}$), critical velocity (v_c), suspended solids concentration, ratio $\overline{V}/v_c$, and shape parameter 'r', the trapping capacity on the dam reservoir on the Lobo River in a tropical region was estimated. The results show that, considering the settling velocity of suspended solids, following the Gamma distribution law remains an innovative solution proposed to evaluate the trapping capacity in water reservoirs. The results show that the mean suspended solids settling velocity $\overline{V}$ is well above the median rate $V_{50\%}$. For a parameter $\overline{V}/v_c \geq 4$, there is an increase in the trapping capacity of the water retention. As established, a large proportion of the sediment is trapped. Furthermore, for a parameter $\overline{V}/v_c \leq 4$, a decrease in the trapping capacity of the Lobo River water reservoir is observed.

Keywords: particle settling velocity; sediment trapping capacity; suspended matter; Gamma distribution law; Lobo River reservoir

1. Introduction

The settling velocity of suspended solids is a crucial parameter in modelling sediment transport in riverine, estuarine, and marine environments. However, quartz particles' falling velocity is easily determined by their size and density, which is only sometimes the case for suspended solids. The point is that the grain size and mineralogical compositions of the discharged particles are unknown [1]. As suspended solids are very fragile, the most appropriate method for determining their sink rate is in situ measurement [2,3]. Two sedimentary phenomena are involved in the suspended solids' fall rate, which is the vertical distribution of suspended solids (SS) and their deposition flux. The settling velocity varies according to the local concentration of suspended sediments (SSC) [4,5]. For dilute suspensions, the settling velocity increases with the SSC. For highly concentrated suspended sediments (SSC > 10 kg/m^3), the settling velocity decreases with increasing SSC (impeded settling velocity). Several methods have been developed in the world to evaluate the falling velocity of suspended matter, namely the setting up of falling velocity tubes for suspended solids by several scientists. According to [6], they made a Quasi In Situ

Settling velocity (QUISSET) tube; the authors of [7] set up a FIeld PIpette WIthdrawal TUbe (FIPIWITU). The authors of [8] developed the BIGDAN settling tube, and [9] developed the Rijkswaterstaat (RWS) field settling tube. Owen [10] developed a method involving a sedimentation tube as a quasi-in situ technique. Successfully used in research [1,11,12], it is a method that involves using a sedimentation rate tube, a quasi-in situ technique. By taking several samples from the bottom of a vertically oriented tube at different times, it is possible to estimate the number of particles deposited at each time interval. Based on of these samples, a distribution of the settling velocity of the suspended solids is obtained. The variation of the fall velocity as a function of concentration SSC is often described by Owen's law [10]. The assessment of the correlation between the fall velocity and the associated concentrations is often of paramount importance [13,14], and only settling tubes are capable of analysing the sedimentation velocities of suspended solids in situ. However, Owen's [10] tube method has been widely criticised because of the disturbance the tube may cause to the flocs during sampling. It appears that the velocities obtained may be an order of magnitude lower than direct measurements compared to the video technique. Nevertheless, a well-established sampling protocol with decantation tubes can give realistic results [6,11,15]. In addition to evaluating the settling tube velocity of suspended solids, there are transport models that allow the estimation of the velocity of suspended solids. According to Dyer [7], Puls and Kühl [8] and Dyer et al. [11] characterise the settling velocity by its median value ($V_{50\%}$). According to the Sanchez theory [2,15], the median fall velocity ($V_{50\%}$) is always lower than the mean settling velocity ($\overline{V}$), which gives a better description of the vertical dynamics of the sediments. Indeed, in many hydrosedimentary models, the fall velocity is represented by a scale, as in Owen's law [4,16,17]. Furthermore, the falling velocity is a stochastic variable due to several different aggregates in suspension simultaneously. Sanchez's approach inspired us, so we used his method [15] for the first time, as it turns out, for a dam reservoir in an equatorial region. To this end, the Lobo River dam reservoir constitutes the first experimental site for this original method. This study deals with the seasonal changes in the distribution and decantation of suspended solids as a function of their fall velocity and trapping capacity in dam reservoirs.

2. Methods and Data

2.1. Study Area

Located in the central-west of Côte d'Ivoire between -6.93° and 6.20° W and between 6.8° and 7.9° N, the Lobo catchment area drains an area of about 7000 km² at Nibéhibé (Figure 1). The catchment of the Lobo reservoir is 5740 km². A monotonous relief characterises its catchment with an altitude ranging between 190 and 612 m.a.s.l. [18]. The reservoir is the main source of drinking water for the city of Daloa. The Lobo River is one of the main tributaries of the Sassandra River on the left bank [19,20]. Its catchment area is not confined to a single administrative entity. Most of the basin covers the districts of Daloa, Vavoua, and Zoukougbeu, and its extreme north belongs to the district of Séguéla. The city of Daloa is the economic hub of the region. It is located about 410 km northwest of Abidjan. It is the third-largest city in Côte d'Ivoire. The climate is equatorial, with a rainy season from March to October and an average annual rainfall of about 1150 mm. The Lobo reservoir was commissioned in 1976 and is the main source of drinking water supply for the population of approx. 0.5 M people of Daloa [21]. From a pedological point of view, the Lobo River catchment has essentially ferralitic soils with a high or medium degree of desaturation. The geological formations in the Lobo catchment area belong mainly to the Precambrian basement (Middle Precambrian) and are grouped into two main entities: magmatic rocks and metamorphic rocks [22].
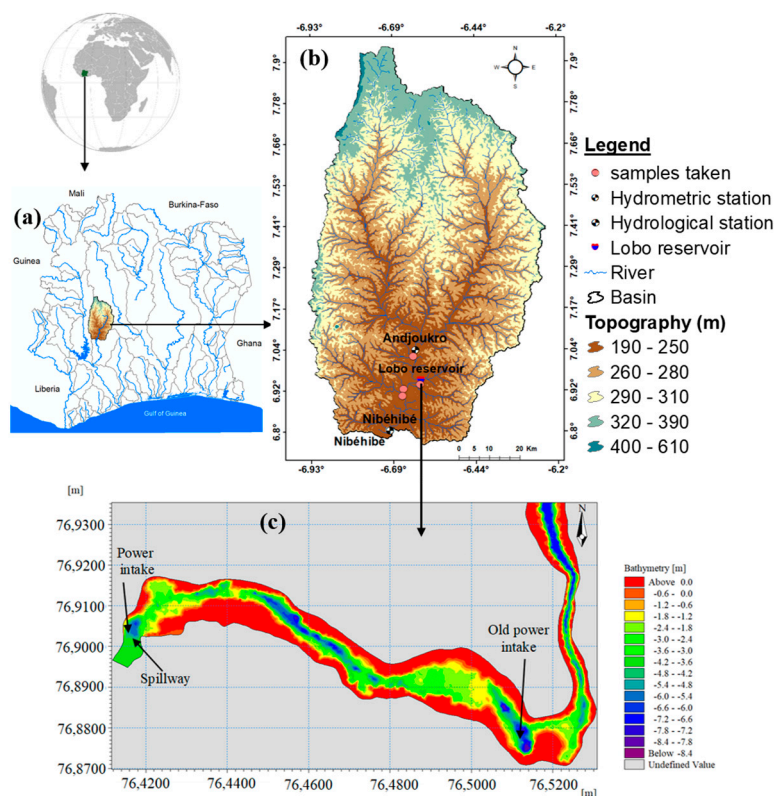
Figure 1. Location of the research area. (**a**) Lobo River basin against the Côte d'Ivoire map. (**b**) Lobo river basin at Nibéhibé. (**c**) Lobo River reservoir.

The characteristics of the Lobo reservoir are summarised in Table 1. The dam's normal water level (231.03 m) is 360,000 m^3. Anthropogenic activities in the catchment are very diverse; however, agriculture remains the main activity of the population.

Table 1. Characteristics of the Lobo Reservoir.

Parameters	Values	Units
Date of commission	1976	
Water inflow	11.18	m^3/s
Water outflow	13.33	m^3/s
Average length of the reservoir (L)	4300	m
Average width of the reservoir (B)	74	m
Average depth	3.5	m
Reservoir area	0.3	km^2
Flow rate drawn	675	m^3/h
Weir length	47	m
Spillway crest elevation	231,033	m
Volume at reservoir elevation	360,000	m^3

2.2. Data

2.2.1. Hydrological Data

The hydrological team of the Environmental Sciences and Technology Laboratory of the Jean Lorougnon Guédé University, Daloa, provided daily water flow data from the Andjoukro-Sikaboutou hydrometric station. This station is located about 8 km upstream of the Lobo River reservoir, and Nibéhibé is about 20 km downstream of the reservoir. The hydrometric data of the stations cover 2019–2020.

2.2.2. Suspended and Bottom Solids Data

In 2019–2020, water samples were collected in the reservoir and at the Andjoukro-Sikaboutou station. The samples were taken in each of the 12 months using a Van Dorn hydrological bottle at different depths (surface, mid-depth, and bottom). The sediment samples were taken upstream, in the reservoir, and after the reservoir in the Lobo River. In the laboratory, the water samples were filtered on a Millipore filtration manifold using pre-weighed WHATMAN GF/F circular filters 47 mm in diameter and 0.45 μm porosity. After drying in an oven at 105 °C, the filters were carefully recovered, and the ratio of the mass of suspended solids to the volume of filtered water samples was used to calculate the SSC [23]. The bed resistance with a Strickler number of 35 $m^{1/3}$/s and a dry density of 500 kg/m^3 was chosen regarding the mean grain size of the sediments sampled.

2.2.3. Methods
Suspension Sediment Discharge

The suspended sediment discharge in the Lobo River reservoir was calculated as follows [23]:

$$Q_{SSC} = Q_L \times SSC \tag{1}$$

where Q_{SSC} is the suspended sediment discharge (kg/s), Q_L is the river flow (m^3/s), and $SSCC$ is the suspended sediment concentration (SSC, kg/m^3).

Configuration of the Mathematical Problem

Modelling of the settling velocity and trapping capacity of the Lobo River reservoir using the theory of settling ponds was developed as part of this study. Two main hypotheses were developed, namely Hypothesis 1: The settling velocity is constant and Hypothesis 2: The settling velocity is distributed according to the Gamma law.

To implement the mathematical model, we used a classical case with cross-sections every fifty metres (50 m) over a distance of 4.3 km. A total of 86 cross-sections were obtained. The reservoir has three distinct zones: the inlet, the deposition, and the outlet zone (after the weir) (Figure 2).
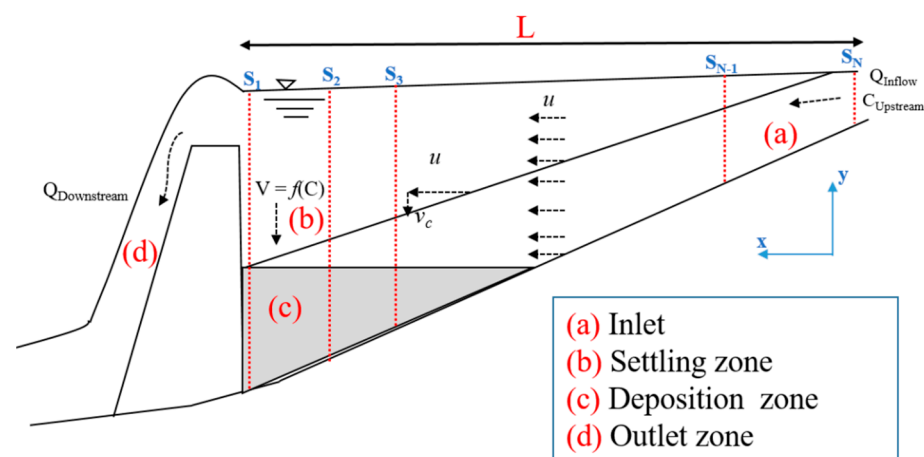

Figure 2. Sketch of the Lobo reservoir with the characteristic zones. Explanations: (a) inlet zone, (b) settling zone, (c) deposition zone, and (d) outlet zone. S1, S2 . . . SN are a cross-section of the Lobo River reservoir.

Two important relationships between the mean flow velocity (U) and the residence time of the sediments in the reservoir (T) are presented:

$$U = \frac{Q}{HB} \tag{2}$$

$$T = \frac{L}{u} = \frac{HBL}{Q} \qquad (3)$$

At the entrance to the settling zone (at x = 0), in most cases, the fluid is homogeneous, and the concentration C(x,y) is constant over the entire depth; therefore, C(0,y) = C_0.

A critical deposition rate vc is defined as follows:

$$v_c = \frac{H}{T} = \frac{uH}{L} = \frac{Q}{BL} \qquad (4)$$

where H is the mean depth of the reservoir, Q is the flow into the reservoir, B is the mean width of the reservoir, L is the mean length of the reservoir, U is the mean flow velocity, and T is the residence time of suspended solids.

Good knowledge of the average depth of the Lobo River reservoir required detailed bathymetry. To this end, bathymetric surveys were carried out on the Lobo River reservoir in 2020 using a single-beam echo sounder (SBES) with a frequency of 450 kHz to allow the waves emitted by the echo sounder not to penetrate the soft sediment [24].

All suspended solids fall with a settling velocity equal to or greater than v_c and settle in the settling zone. For suspended solids, falling with a settling velocity of less than v_c, deposition occurs only for particles below the level h = vT at the entrance to the settling zone. Generally, the trapping capacity (η) of a settling tank depends on the turbulence and the statistical distribution of falling velocities associated with each suspended particle.

Experimental Study of the Settling Velocity in Situ in a Sedimentation Tube

Twelve tests (twelve months) were carried out on water samples taken from the surface, mid-depth, and at the bottom of the water column to study the settling velocity distribution under still water conditions. The local distribution of suspended solids in terms of the settling velocity was examined by the Owen tube method. The Owen [10] tube is positioned vertically. Samples of one-tenth of the initial volume are then taken from the bottom of the tube at different times. The samples are distributed over time to differentiate speed groups and estimate the number of particles settling at each interval (2 min, 4 min, 8 min, 15 min, 30 min, 60 min, 120 min, 240 min, and 480 min). Finally, a last sample is taken to recover the remaining liquid in the tube to estimate the overall solid mass of the sample. The SSC was then determined after filtration of the water sample's filtration manifold using pre-weighed WHATMAN GF/F circular filters 47 mm in diameter and 0.45 μm porosity. After being dried at 105 °C, the filters were carefully recovered and marked to determine the total SSC expressed in kg/m^3 [25]. A distribution curve representing the percentage by weight $V(\%)$ of grains with a settling velocity lower than $V_d = H/t$, where H is the fall height of the sediment and t is the sedimentation time measured from the beginning of the test, was drawn. The median settling velocity $V_{50\%}$ and the settling velocity $V_{90\%}$ are obtained from the settling velocity distribution function curves. The settling velocity V of the suspended solids is studied as a stochastic variable. According to Sanchez [2], the settling velocity follows a probability law following the Gamma law with a shape parameter r that characterises the range of values of the fall velocity for all the aggregates simultaneously in suspension. All suspended particles fall with a variable settling velocity, depending on their concentrations and weights.

Modelling the Trapping Capacity of a Reservoir

Suspended Solids with a Constant Settling Velocity

The near-bottom concentration remains constant until the total settling of the suspended solids if a continual settling velocity and no mixing in the Lobo River reservoir is considered. This case is discussed below.

Constant settling velocity and no turbulence (CV-NT model)

In still water conditions, the concentration in the settling zone of the Lobo River reservoir is given by Sanchez [26]:

$$
C(x,y) = \begin{cases} 0 & for : \left(1 - \frac{\overline{V} \times x}{u \times H}\right) H < y < H \\ C_0 & for : 0 \leq y \leq \left(1 - \frac{\overline{V} \times x}{u \times H}\right) H \end{cases}
\tag{5}
$$

As a function of x, the solid mass M remaining in suspension in the water column is:

$$
M(x) = \begin{cases} \left(1 - \frac{\overline{V} \times x}{u \times H}\right) H C_0 & for : x \leq \frac{u \times H}{\overline{V}} \\ 0 & for : x > \frac{u \times H}{\overline{V}} \end{cases}
\tag{6}
$$

The trapping capacity is:

$$
\eta = \frac{M(0) - M(L)}{M(0)} = \begin{cases} \frac{\overline{V}}{v_c} & for : \overline{V} \leq v_c \\ 1 & for : \overline{V} > v_c \end{cases}
\tag{7}
$$

- **Constant settling velocity with complete mixing (CV-CM model)**

Many analytical solutions can be proposed to describe the diffusion produced by turbulence [27,28]. By assuming a perfect vertical mixing, for each variable x, the concentration is constant on y ($C(x,y) = \overline{C}(x)$, where $\overline{C}(x)$ is the local mean vertical concentration. For an observer moving through the settling zone with the same velocity u as the horizontal flow, the variation of the SSC is presented [26]:

$$
\left. \frac{dM(x)}{dt} \right|_{following\ the\ horizontal\ flow} = \left. \frac{d(H \times \overline{C}(x))}{dt} \right|_{following\ the\ horizontal\ flow} = -\overline{V} \times \overline{C}(x)
\tag{8}
$$

Then, the variation on x of $\overline{C}(x)$ is governed by:

$$
\frac{d\overline{C}(x)}{dx} = -\frac{\overline{V}}{uH} \times \overline{C}(x)
\tag{9}
$$

And the solution is:

$$
\overline{C}(x) = \overline{C}(0) \exp\left(-\frac{\overline{V} \times x}{u \times H}\right)
\tag{10}
$$

As a function of x, the solid mass M remaining in suspension in the water column is:

$$
M(x) = H\overline{C}(0) \exp\left(-\frac{\overline{V} \times x}{u \times H}\right)
\tag{11}
$$

The trapping capacity is:

$$
\eta = \frac{M(0) - M(L)}{M(0)} = 1 - \exp\left(-\frac{\overline{V}}{v_c}\right)
\tag{12}
$$

- **Suspended Solids with Varying Settling Velocities**

The second approach of this study is to consider the settling velocity V of suspended solids as a stochastic variable. According to Sanchez [2], the settling velocity follows a probability law similar to the Gamma distribution, with a shape parameter "r" that describes the range of values of the fall velocity for settling aggregates simultaneously in suspension. All suspended particles fall with a variable settling velocity, depending on their concentrations and weights. A similar approach was developed by Sanchez [2] to describe cohesive sediments and Khawaja [29] for non-cohesive sediments. The shape parameter r (invariant during the settling process) and the average settling velocity (increasing with the concentration of suspended solids) allow defining the Gamma distribution law (Figure 3).
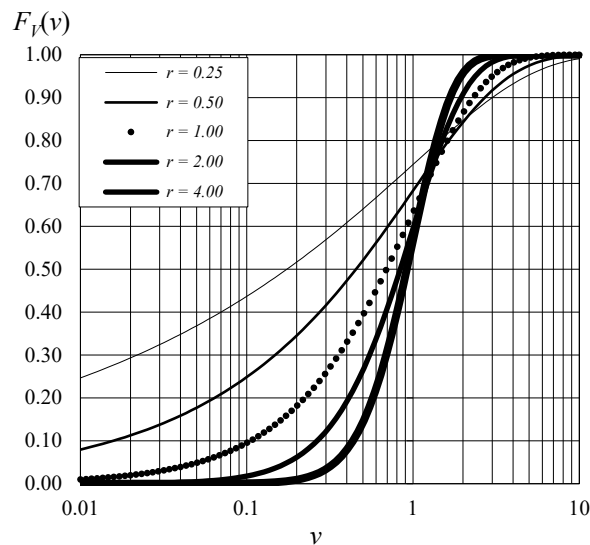
$F_V(v)$

Figure 3. Suspended solids settling velocity distribution function for five values of the parameter r [26].

The settling velocity of a suspended matter component of infinitesimal unit mass *dm* is defined as a random variable *V*. The probability density function (*pdf*) of *V* for a sample of suspended matter as a function of the parameters *v* of *V* is given by *fV(v)*. *fV(v)*d*v* represents the quantity of matter by unit volume. The values of *V* are between *v-dv/2* and *v + dv/2*. The probability density function is given by:

$$F_V(v) = \int_0^v f_V(v)\,dv \tag{13}$$

Field measurements allowed fitting a probability density function of V. For natural sediments, *fV(v)* is well described by Gamma distribution. Indeed, several probability density laws can be used to model the distribution of the velocities of settling materials, but Gamma distribution is the one that most closely approximates reality [15,16]:

$$f_V(v) = \frac{\lambda^r\,v^{r-1}\,\exp(-\lambda\,v)}{\Gamma(r)}, \quad 0 \le v < \infty \tag{14}$$

Γ is a Gamma function. The parameters *r* and λ are dependent on the mean settling velocity $\overline{V}$ and the standard deviation σ of the values of *V* [26]:

$$r = \frac{\overline{V}^2}{\sigma^2}, \; \lambda = \frac{\overline{V}}{\sigma^2} = \frac{r}{\overline{V}} \tag{15}$$

As the fluid is homogeneous throughout the depth at the entrance to the Lobo River reservoir (X = 0), the probability density function of *V* is assumed to be vertically invariant.

- **Varying settling velocity and no turbulence (VV-NT model)**

All particles with a settling velocity V > V' = H/t are deposited after a time *t* (from height *H*). Aggregates with settling velocities lower than V' are also deposited (variable height $V \times t \le H$). The proportion of sediment remaining in suspension is described by [1,6]:

$$P = \frac{M(x = ut)}{M(0)} = \int_0^{V'} \left(1 - \frac{v\,t}{H}\right) f_V(v)\,dv \tag{16}$$

The Gamma law is calculated as follows:

$$\int\limits_{0}^{V'} \frac{v\,T}{H} f_V(v)\,dv = \frac{T}{H}\int\limits_{0}^{V'} v\,\frac{\lambda^r\,v^{r-1}\,\exp(-\lambda v)}{\Gamma(r)}\,dv,\tag{17}$$

With $\alpha - 1 = r$, the result is:

$$\int\limits_{0}^{V'} \frac{v\,T}{H} f_V(v)\,dv = \frac{T}{H}\,\frac{\lambda^r}{\lambda^{r+1}}\,\frac{\Gamma(r+1)}{\Gamma(r)}\int\limits_{0}^{V'} \frac{\lambda^\alpha\,v^{\alpha-1}\,\exp(-\lambda v)}{\Gamma(\alpha)}\,dv,\tag{18}$$

As $(r+1)/(r) = r$ and $\overline{V} = r/\lambda$:

$$\int\limits_{0}^{V'} \frac{v\,T}{H} f_V(v)\,dv = \frac{T}{H}\times\overline{V}\int\limits_{0}^{V'} \frac{\lambda^\alpha\,v^{\alpha-1}\,\exp(-\lambda v)}{\Gamma(\alpha)}\,dv\tag{19}$$

An observer moving with the flow from $x = 0$ to time $t = 0$, the two parameters are linked by $x = ut$, so the formula for P becomes [26]:

$$P = \int\limits_{0}^{V'/\overline{V}} \frac{r^r\,(v^*)^{r-1}\,\exp(-rv^*)}{\Gamma(r)}\,dv^* - \frac{uT}{L}\times\frac{\overline{V}}{v_c}\int\limits_{0}^{V'/\overline{V}} \frac{r^\alpha\,(v^*)^{\alpha-1}\,\exp(-rv^*)}{\Gamma(\alpha)}\,dv^*\tag{20}$$

The trapping capacity is:

$$\eta = \frac{M(0)-M(L)}{M(0)} = 1 - \int\limits_{0}^{v_c/\overline{V}} \frac{r^r\,(v^*)^{r-1}\,\exp(-rv^*)}{\Gamma(r)}\,dv^* + \frac{\overline{V}}{v_c}\int\limits_{0}^{v_c/\overline{V}} \frac{r^\alpha\,(v^*)^{\alpha-1}\,\exp(-rv^*)}{\Gamma(\alpha)}\,dv^*\tag{21}$$

With $\overline{V}$ is the mean settling velocity of the suspended solids. The expression η was evaluated by using a Gamma distribution probability calculator; v^* is a non-dimensional settling velocity; and as $\Gamma\,(r+1)/\Gamma\,(r) = r$, and $\overline{V} = r/\lambda$.

- **Varying settling velocity with complete mixing (VV-CM model)**

Under the assumption of perfect vertical mixing, when at each x, the concentration is constant over y ($C(x,y) = \overline{C}(x)$), and the variation over x of $\overline{C}(x)$ is described by:

$$\frac{d\overline{C}(x)}{dx} = -\frac{\overline{V}}{uH}\times\overline{C}(x)\tag{22}$$

During the settling of the suspended solids, the average settling velocity decreases with the concentration of the suspended solids. This variation was demonstrated by [2]:

$$\overline{V}(x) = \overline{V}(0)\times\left(\frac{\overline{C}(x)}{\overline{C}(0)}\right)^{\frac{1}{r}}\tag{23}$$

Using Equations (22) and (23), we can obtain the following:

$$\frac{d\overline{C}(x)}{dx} = -\frac{\overline{V}(0)}{u\times H\times\overline{C}(0)^{\frac{1}{r}}}\times\overline{C}(x)^{\frac{1+r}{r}}\tag{24}$$

The solution for $\overline{C}(x)$ is:

$$\frac{C(x)}{C(0)} = \left(\frac{r\times u\times H}{r\times u\times H + \overline{V}(0)\times x}\right)^r\tag{25}$$

The trapping capacity is:

$$\eta = \frac{M(0) - M(L)}{M(0)} = 1 - \left(\frac{r}{r + \overline{V}(0)/v_c}\right)^r \tag{26}$$

where $\overline{V}(0)$ is the mean settling velocity of the suspended solids at $x = 0$.

The implementation of the model required the calculations of several additional parameters: Local coefficient of friction:

$$C_f = \frac{2 \times g}{K^2{}_s \times H^{1/3}} \tag{27}$$

Shear rate:

$$U^* = \left(\frac{C_f}{2}\right)^{1/2} \times U \tag{28}$$

where K_s is the Strickler coefficient, U is the flow velocity, and H is the average depth of the water reservoir, U^* is the shear velocity.

3. Results

3.1. SSC in Lobo River Reservoir

Table 2 shows the suspended solids' monthly and annual inputs into the Lobo River reservoir. The SSC are between 0.0105 and 0.031 kg/m^3 for an annual average concentration of 0.016 kg/m^3. The concentrations evolve according to the flow rates of the Lobo River. Solid inputs are higher in the dry season than in the rainy season, because flows are higher during this period. During the dry season, particulate flows range from 20.3 t to 75 t. During the rainy season, particle flows range from 58.3 t to 4815.8 t. During the hydrological cycle, the reservoir received approximately 9744.1 t of suspended matter, of which 8905.2 t exited downstream. The overall annual balance of the inflow and outflow of these suspended solids flows shows that the Lobo River reservoir retained approximately 838.9 t (8.6%) of suspended solids.

Table 2. Suspended sediment discharge balance for the Lobo River reservoir.

	Jan	Feb	Mar	Apr	May	Jun	Jul	Aug	Sep	Oct	Nov	Dec	Annual Average
Inflow (m^3/s)	0.98	0.77	1.21	3.32	2.8	10.5	9.34	16.5	40	58	15.3	2.8	13.458
SSL$_{in}$ (kg/m^3)	0.011	0.011	0.018	0.018	0.015	0.013	0.012	0.016	0.025	0.031	0.013	0.010	0.016
Outflow (m^3/s)	1.30	1.76	4.69	6.62	10.63	12.65	13.50	17.05	35.70	45.00	17.20	5.32	14.283
SSL$_{out}$ (kg/m^3)	0.01	0.01	0.02	0.02	0.01	0.01	0.01	0.01	0.02	0.03	0.01	0.07	0.019
Average (kg/m^3)	0.011	0.010	0.017	0.017	0.014	0.012	0.013	0.014	0.022	0.030	0.012	0.040	0.018
Inflow sediment discharge (t)	29.9	20.3	58.3	155.8	113.2	360.9	300.2	707.1	2592.0	4815.8	515.5	75.0	9744.1
Outflow sediment discharge (t)	34.7	44.0	188.2	274.5	370.0	327.9	470.1	548.0	1665.6	3495.3	490.4	996.5	8905.2
Budget (t)	−4.8	−23.7	−129.9	−118.8	−256.7	33.1	−170	159.1	926.4	1320.5	25.1	−921.5	838.9

3.2. Hydrodynamic Parameters of the Models

The hydrodynamic parameters of the Lobo River during our research are presented in Table 3. The results show that the parameters vary monthly and depend strongly on the liquid flow entering the reservoir. During the low water period, the flows are very low and vary between 0.77 and 2.8 m^3/s, with a critical particle velocity between 2.41986×10^{-6} m and 8.8×10^{-6} m. However, during the flood period, the critical particle velocity is between 4×10^{-6} m/s and 0.00018 m/s. The particles tend to be deposited during a flood when solid inputs and velocity currents are higher.

Table 3. Hydrodynamic parameters of the Lobo reservoir models.

	Jan	Feb	Mar	Apr	May	Jun	Jul	Aug	Sep	Oct	Nov	Dec
Q	0.98	0.77	1.21	3.32	2.8	10.47	9.34	16.5	40	58	15.3	2.8
B (m)	74	74	74	74	74	74	74	74	74	74	74	74
L (m)	4300	4300	4300	4300	4300	4300	4300	4300	4300	4300	4300	4300
H (m)	2.012	1.98	2.31	2.55	2.66	2.88	2.74	2.93	3.875	3.5	3.38	2.18
v_c (m/s)	3×10^{-6}	2.4×10^{-6}	4×10^{-6}	1×10^{-5}	8.8×10^{-6}	3.3×10^{-5}	2.9×10^{-5}	5.2×10^{-5}	0.00013	0.00018	4.8×10^{-5}	8.8×10^{-6}
K_s (m$^{1/3}$ s^{-1})	35	35	35	35	35	35	35	35	35	35	35	35
C_f (Ks^{2}d$^{1/3}$)	0.0127	0.0128	0.0121	0.0117	0.0116	0.0113	0.0114	0.0112	0.0102	0.0105	0.0107	0.0124
U_{moy} (m/s)	0.00658	0.00526	0.00708	0.01759	0.01422	0.04913	0.04606	0.07610	0.13949	0.22394	0.06117	0.01736
U^* (m/s)	0.0005	0.0004	0.0006	0.0013	0.0011	0.0037	0.0035	0.0057	0.0100	0.0163	0.0045	0.0014
V_{moy}/v_c	34.71	38.10	37.61	13.45	14.74	3.56	3.76	2.62	1.09	1.15	2.47	10.41

U^* is the shear velocity.

3.3. Function of Distributing the Settling Velocity of Suspended Solids

The results of the different distribution functions of suspended solids as a function of the particle settling velocity for twelve settling column tests carried out in the laboratory are presented in Figure 4. It can be seen that there is a good distribution of suspended solids. The particle settling velocity increases with the concentration. Most of the curves obtained are similar: they have the same profile and the same trend, but each speed corresponds to a particle size. The curves migrate downwards from a low concentration to a higher concentration, increasing the settling velocity and the settling particles' mass. The differentiation of the settling velocities by class makes it possible to draw the distribution curves of the suspended matter according to their settling velocities. Thus, the median fall velocity $V_{50\%}$ and the settling velocity $V_{90\%}$ are obtained from the suspended matter distribution function curves. Overall, the suspended solids distribution functions vary from month to month. This spatial variation of the sediments shows that the vertical distribution of suspended solids in the Lobo River can be considered gradually varied over time.
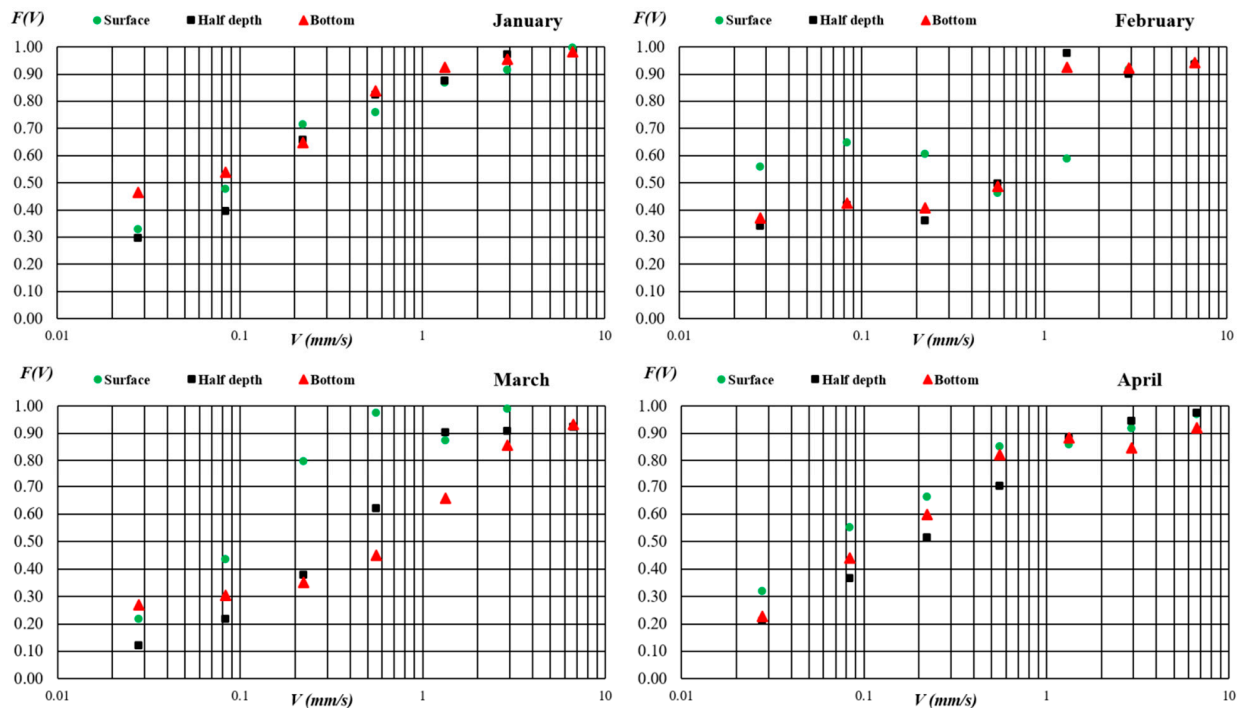

Figure 4. *Cont.*
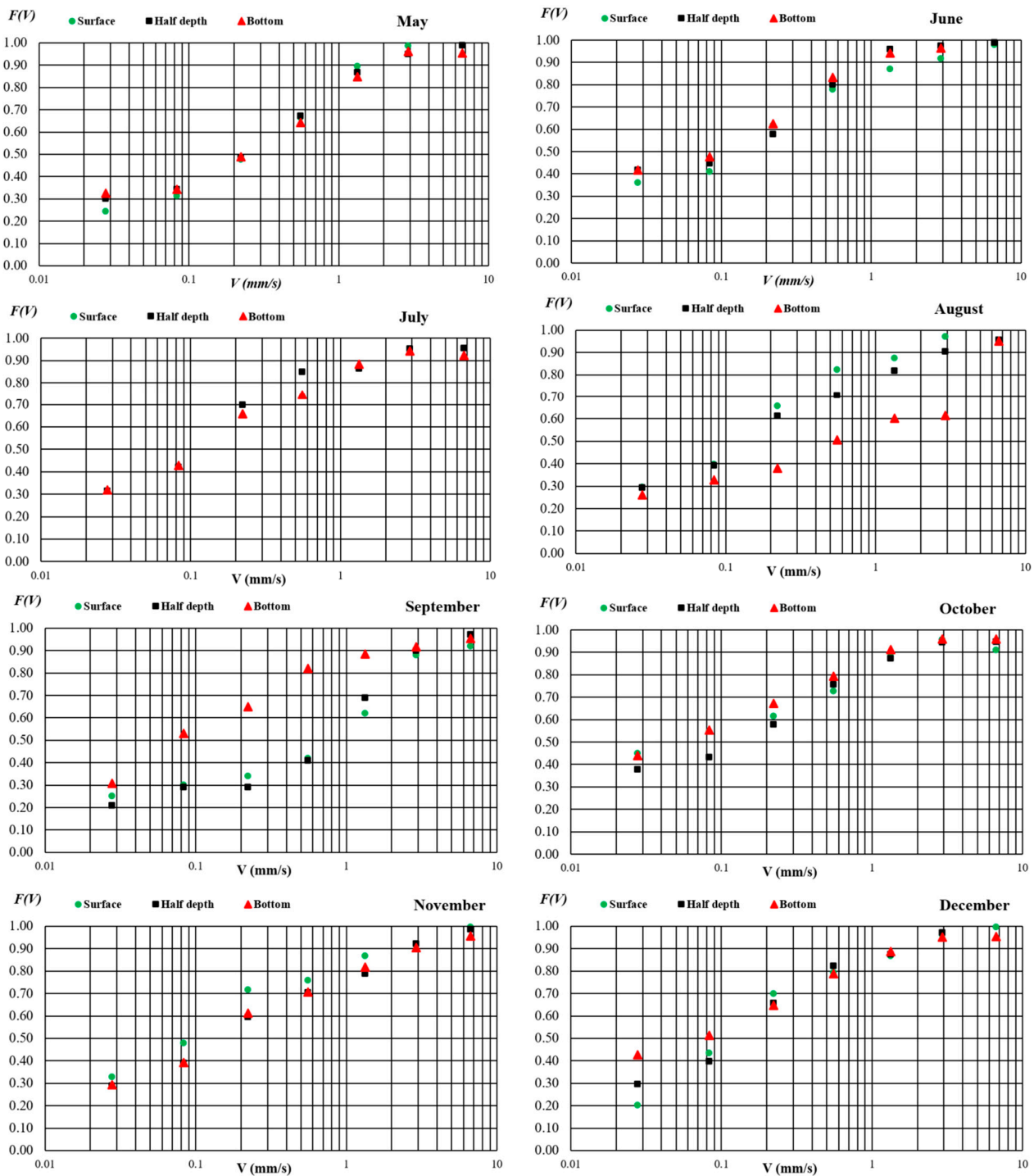
Figure 4. Suspended solids settling velocity distribution functions characteristic of the Lobo reservoir from January to December 2020.

3.4. Variation of the Settling Velocity and Function of the Shape Parameter

After the Owen tube tests, an analysis of the water samples gave mean settling velocities ($\overline{V}$) well above the median fall velocities ($V_{50\%}$), with a variable distribution of r form parameters for each month. The settling velocities vary according to the months and the water inflow in the reservoir. At the beginning of the rainy season (March), there is an increase in the settling velocity of the order of 0.143 mm/s, followed by a decrease in the fall velocity during April, May, June, and July between 0.126 and 0.14 mm/s. The maximum fall velocity (0.221 mm/s) is observed during October (Table 4). The variation of the settling

velocity is also confirmed by the shape parameter '*r*' of the Gamma law, which characterises the settling velocity distribution as a function of the concentration of suspended matter in the water column. The shape parameter r ranges from 0.46 to 1.04, with a median settling velocity significantly lower (0.055–0.075 mm/s) than the average settling velocity of the suspended solids. The shape parameter r varies from month to month.

Table 4. Mean settling velocity of suspended solids as a function of the shape parameter *r* characteristic of the Lobo reservoir in 2020.

Months	r	$1/r$	$\sigma = \dfrac{\underline{V}}{V}$	$\dfrac{V_{90\%}}{V_{50\%}}$	$\dfrac{\overline{V}}{V_{50\%}}$	$V_{50\%}$	$\overline{V}$ (*mm/s*)
January	0.58	1.72	1.31	5.09	1.94	0.055	0.107
February	1.04	0.96	0.98	3.23	1.42	0.065	0.092
March	0.48	2.07	1.44	6.19	2.27	0.063	0.143
April	0.50	1.99	1.41	5.93	2.19	0.064	0.140
May	0.51	1.96	1.40	5.83	2.16	0.060	0.130
June	0.55	1.81	1.34	5.35	2.02	0.058	0.117
July	0.57	1.75	1.32	5.18	1.97	0.064	0.126
August	0.48	2.07	1.44	6.17	2.26	0.060	0.136
September	0.46	2.16	1.47	6.47	2.36	0.058	0.137
October	0.50	2	1.42	6.00	2.21	0.100	0.221
November	0.84	1.19	1.09	3.73	1.55	0.075	0.117
December	1.02	0.98	0.99	3.28	1.43	0.064	0.092

3.5. Settling Velocity as a Function of Concentration

We found that the faster the suspended particles settle, the larger the diameter of the aggregates. In other words, the rate of the fall of suspended matter in the Lobo River increases with the concentration (Figure 5). The dissolved material only settles when it forms aggregates through the phenomenon of flocculation. It is important to note that this same trend is observed in all fine sediments, but the relationship between the sink rate and concentration varies from one sediment to another. The relationship between the sink rate and suspended solids concentration is quite significant. This significance is justified by a very high coefficient of determination (R^2) of 0.9083.
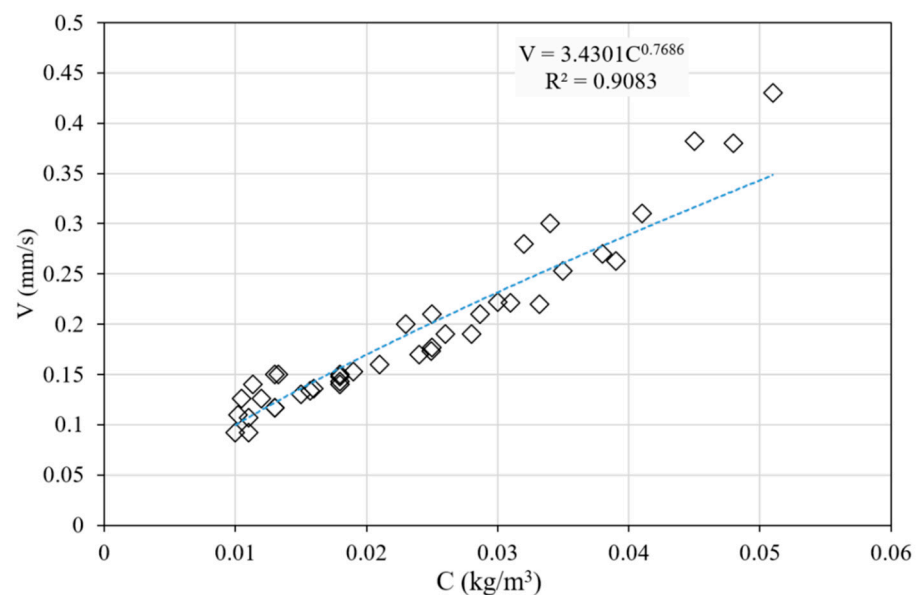

Figure 5. Variation of the settling velocity with SSC on the Lobo reservoir.

3.6. Sediment Trapping Capacity of the Reservoir

The trapping capacity of the Lobo River reservoir depends on the turbulence, critical velocity, suspended solids fall rate, shape parameter r, and the ratio $\overline{V}/v_c$, which is a parameter of the models. The trapping capacity of the reservoir as a function of parameter $1/r$ is presented in Figure 6. Under the assumption of a constant head velocity, in the absence of the turbulence of suspended solids with $\overline{V}/v_c \geq 4$, almost all sediments ($\eta = 0.98$ and $\eta = 1$) tend to be trapped by the Lobo River reservoir. During the low-water period (January, February, and December), in the absence and with turbulence, it is observed that about 100% of the sediments are trapped. During the flood period (August, September, and October), a decrease in the percentage ($\eta = 0.97$ and $\eta = 0.5$) of trapped sediments is observed as a large proportion of the sediments passing over the weir of the reservoir.
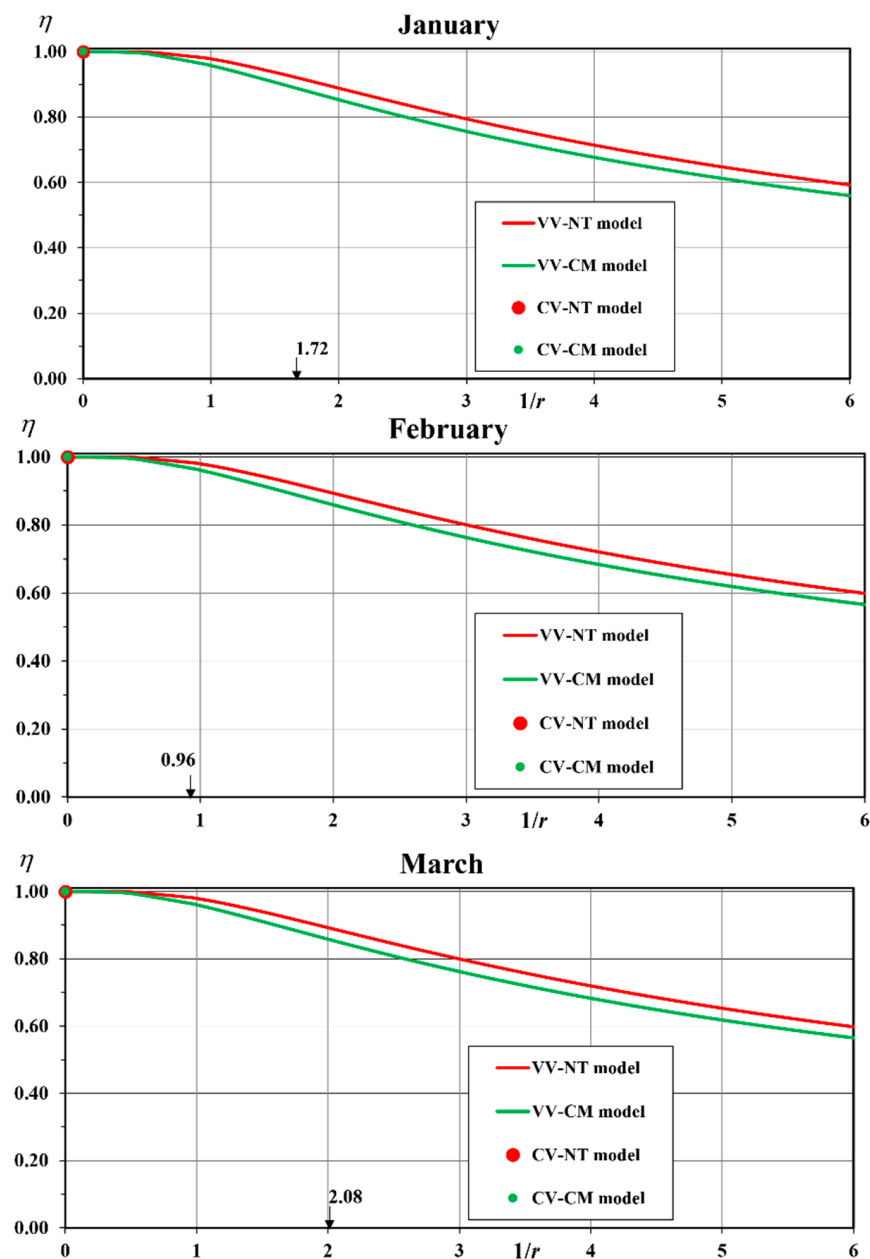
Figure 6. *Cont.*
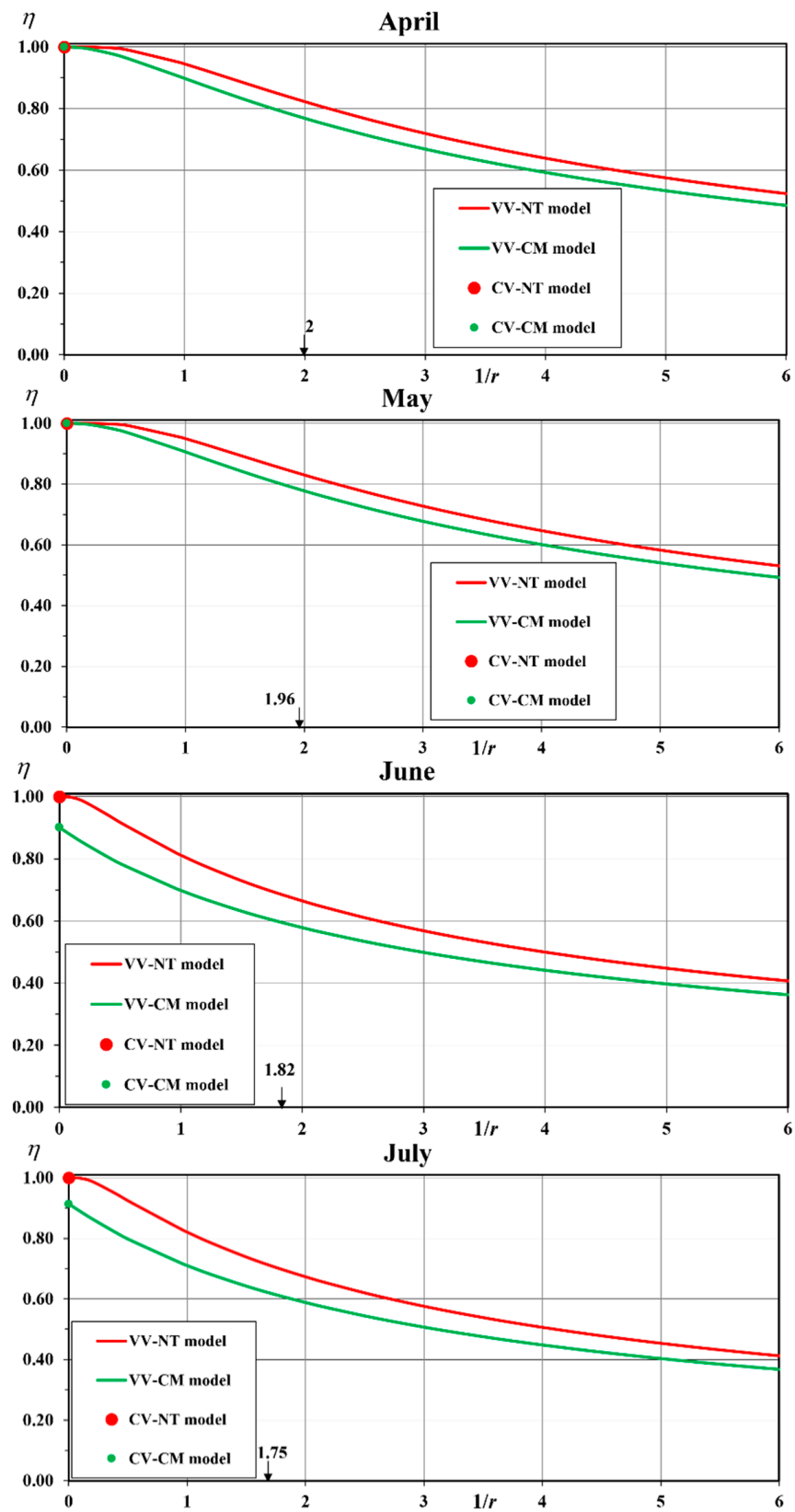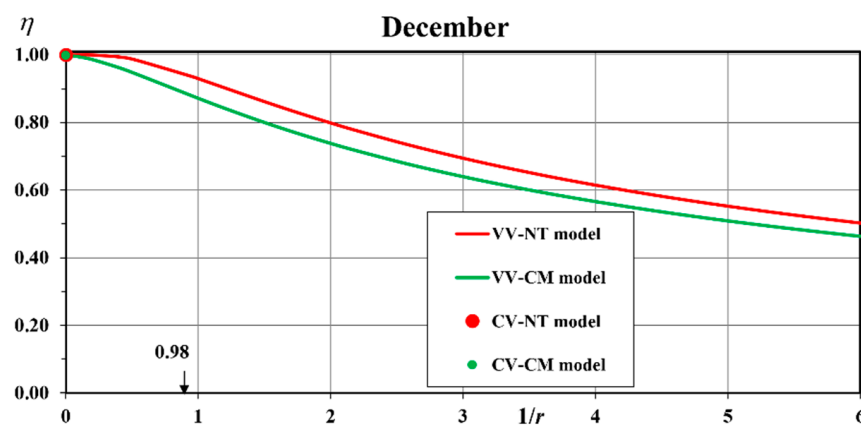
Figure 6. *Cont*.
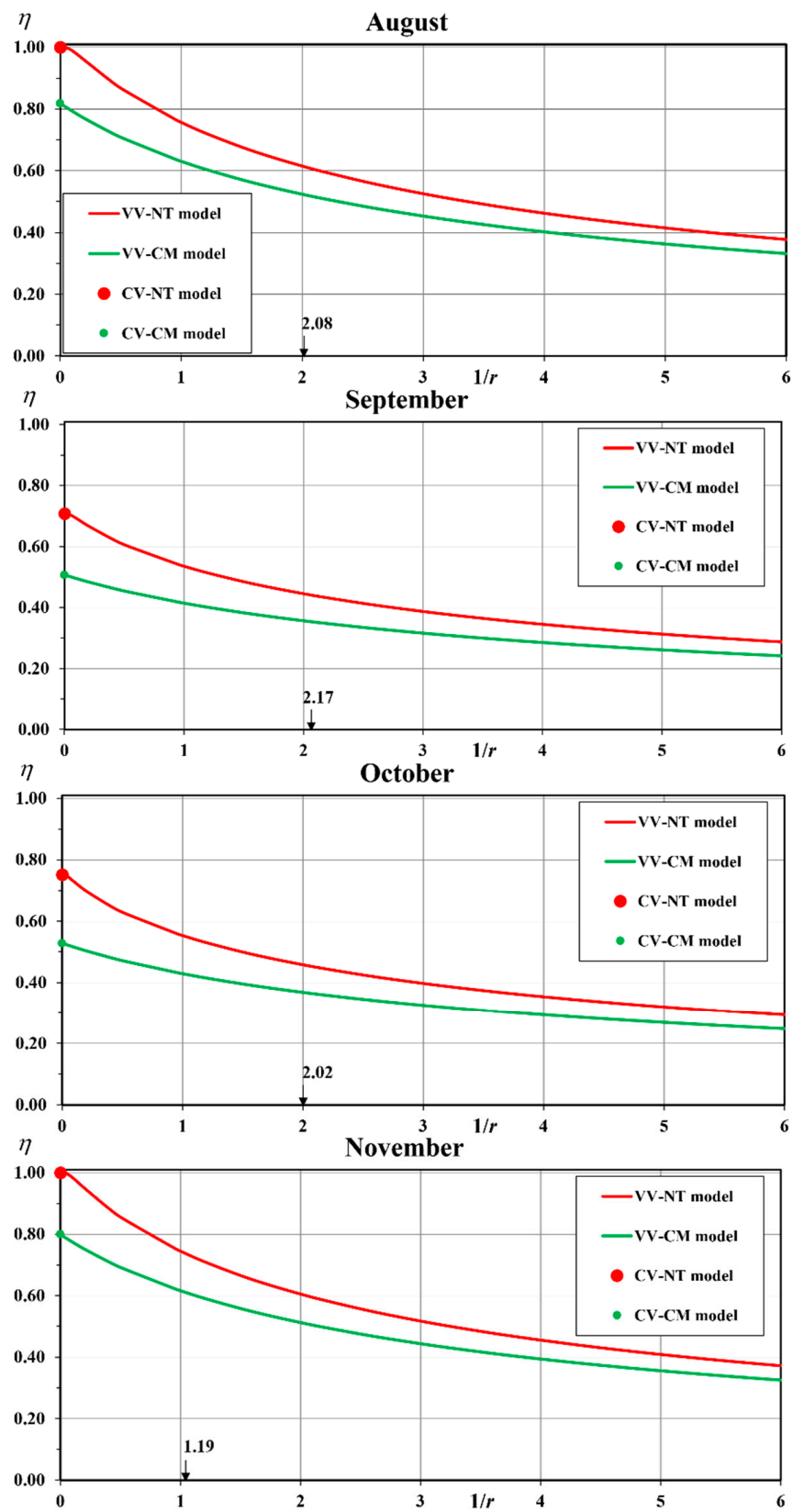
Figure 6. *Cont.*

Figure 6. Annual trapping capacity (η) of the Lobo reservoir.

Under the assumption of a variable head velocity, a decrease in the trapping capacity of the Lobo River reservoir is observed during both the dry and wet periods. In the dry period, the trapping capacity of the reservoir is between $\eta = 0.88$ and $\eta = 0.96$. A drastic decrease in trapped sediments is observed during the flood periods. The ratio of trapped sediment ranges from $\eta = 0.8$ to $\eta = 0.37$ for values of $1/r$ between 1.19 and 2.17. A large proportion of the sediment passes over the weir. Indeed, during this period, the liquid and solid inputs from the river are essential, and a large quantity of sediment is not trapped by the reservoir but passes over the weir. The increase in inflow is accompanied by an increase in sediment transport, which accelerates the silting of the reservoir, reducing its storage capacity.

4. Discussion

Based on the field campaigns on the Lobo River, the estimated solid inputs to the reservoir show that the reservoir receives about 9460.49 t of sediment per year. During the dry season, the inputs range from 20.3 to 75 t. In contrast, during the high-water period, the inflow is between 58.3 and 4815.8 t. This could be explained by the fact that the flows carry a lot of sediment during the rainy seasons due to higher liquid inputs [30–33]. There is an increase in the SSC at the beginning of the rainy season (March) of around 0.018 kg/m^3. This variability could be explained by the variation in vegetation cover (bare soil) and the aggressive nature of the first rains at the beginning of the rainy season [34]. However, Bouguerra [35,36] and Orton [4] reported that the magnitude and nature of suspended solids flows are related, on the one hand, to the intensity of runoff water erosion and, thus, to the amount of rainfall, and on the other hand, to the capacity of the runoff to transport solids. There is a strong correlation between the variations in the suspended solids load and variations in the liquid inputs [37–39]. The suspended solid loads in the Lobo River reservoir (0.018 kg/m^3) are relatively higher compared to the solid loads obtained by Kouassi [40] and Mèlèdje [33–38] in Lake Taabo (0.012 kg/m^3) and Lake Ayamé 1 (0.00615 kg/m^3). This difference could be explained by the degradation of the vegetation cover and the slope's regular inclination, which increases the soil's vulnerability to erosion in the Lobo catchment at Nibéhibé. A suspended matter distribution function obtained the fall velocity. This function shows that the fall velocity varies proportionally with the concentration of suspended solids. Indeed, laboratory measurements have shown that suspended matter's falling velocity and silt cream's settling velocity vary mainly with the concentration, according to laws specific to each sediment [4,16,17]. The results show that the median fall velocity is significantly lower than the mean fall velocity. According to Sanchez [15], this variation in velocity could be due to the phenomenon of turbulence, which increases with the falling velocity of the suspended matter. Four original models were developed to estimate the concentration from a reference concentration and the

trapping capacity in the Lobo River reservoir located in the equatorial zone under two main assumptions:

Assumption 1: Constant fall rate with or without mixing in the reservoir.

Assumption 2: Gamma-distributed head velocity with or without turbulence in the reservoir.

Under the assumption of a constantly suspended solids fall velocity, with a parameter $\overline{V}/v_c \geq 4$, an increase in the trapping capacity of the water reservoir is observed. A large proportion of the sediment is trapped. Furthermore, with the parameter $\overline{V}/v_c \leq 4$, a decrease in the trapping capacity of the Lobo River water reservoir is observed. The reduction in the trapping capacity of the water reservoir could be due to the turbulence phenomenon that leads to the resuspension of particles that are expelled downstream of the weir, thus reducing the efficiency of the reservoir [41,42]. According to Sanchez [26] and Schmidt [43], this decrease in the Lobo River reservoir trapping capacity could be due to flocculation and the high variability in the rate of fall of suspended particles in the water column. The percentage of sediment trapped during the high-water period ($\eta = 0.37$ and $\eta = 0.8$) remains relatively lower than during the dry season ($\eta = 0.88$ and $\eta = 0.96$). This can be explained by the fact that a good proportion of the sediment passes over the weir with very high solid inputs during the high-water period.

5. Conclusions

This original study on the Lobo River reservoir in the equatorial region allowed the understanding of the final settling process and the trapping capacity of suspended solids under two main hypotheses (constant settling velocity and the Gamma law distributed settling velocity). Considering a variable fall velocity of suspended solids by the Gamma distribution law remains an innovative solution proposed to study the trapping capacity in water reservoirs. Using essential parameters, such as flow rate, mean settling velocity ($\overline{V}$), critical velocity (v_c), suspended solids concentration, ratio $\overline{V}/v_c$, and shape parameter 'r', the trapping capacity of the Lobo River reservoir was estimated. For the parameter $\overline{V}/v_c \geq 4$, an increase in the trapping capacity of the water reservoir is observed. A large proportion of the sediment is trapped. Furthermore, for parameter $\overline{V}/v_c \leq 4$, a decrease in the trapping capacity of the Lobo River water reservoir is observed. There is an increase in the trapping capacity of the Lobo River reservoir during the low-water period compared to the flood period. However, the low-water period is marked by a decrease in solid contributions, unlike the flood period. During this period, minimal sediment passes over the reservoir's spillway, because hydrodynamic activities and liquid inputs are relatively low. This gives the reservoir a high capacity to trap the maximum amount of sediment. The study of the impact of the parameters $\overline{V}/v_c$, mean settling velocity ($\overline{V}$), and shape parameter 'r' on the thickness of the deposits in the Lobo River reservoir could be the subject of future studies. It is important to stress that the original methodology proposed in this study can be used in all regions of the world.

References

1. Malarkey, J.; Jago, C.; Hübner, R.; Jones, S. A simple method to determine the settling velocity distribution from settling velocity tubes. *Cont. Shelf Res.* **2013**, *56*, 82–89. [CrossRef]
2. Sánchez, M.; Grimigni, P.; Delanoë, Y. Steady-state vertical distribution of cohesive sediments in a flow. *Comptes Rendus Geosci.* **2005**, *337*, 357–365. [CrossRef]
3. Xiao, L.; Hu, Y.; Greenwood, P.; Kuhn, N.J. A Combined Raindrop Aggregate Destruction Test-Settling Tube (RADT-ST) Approach to Identify the Settling Velocity of Sediment. *Hydrology* **2015**, *2*, 176–192. [CrossRef]
4. Orton, P.; Kineke, G. Comparing Calculated and Observed Vertical Suspended-Sediment Distributions from a Hudson River Estuary Turbidity Maximum. *Estuar. Coast. Shelf Sci.* **2001**, *52*, 401–410. [CrossRef]
5. Tarpley, D.R.; Harris, C.K.; Friedrichs, C.T.; Sherwood, C.R. Tidal Variation in Cohesive Sediment Distribution and Sensitivity to Flocculation and Bed Consolidation in An Idealized, Partially Mixed Estuary. *JMSE* **2019**, *7*, 334. [CrossRef]
6. Jones, S.; Jago, C. Determination of settling velocity in the Elbe estuary using quisset tubes. *J. Sea Res.* **1996**, *36*, 63–67. [CrossRef]
7. Cornelisse, J.M. The field pipette withdrawal tube (FIPIWITU). *J. Sea Res.* **1996**, *36*, 37–39. [CrossRef]
8. Puls, W.; Kühl, H. Settling velocity determination using the BIGDAN settling tube and the Owen settling tube. *J. Sea Res.* **1996**, *36*, 119–125. [CrossRef]
9. van Leussen, W. The RWS field settling tube. *J. Sea Res.* **1996**, *36*, 83–86. [CrossRef]
10. Owen, M.W. *Determination of the Settling Velocities of Cohesive Muds*; Hydraulic Research Station IT: Wallingford, UK, 1976; p. 161.
11. Dyer, K.; Cornelisse, J.; Dearnaley, M.; Fennessy, M.; Jones, S.; Kappenberg, J.; McCave, I.; Pejrup, M.; Puls, W.; Van Leussen, W.; et al. A comparison of in situ techniques for estuarine floc settling velocity measurements. *J. Sea Res.* **1996**, *36*, 15–29. [CrossRef]
12. Koffi, B.; Kouassi, K.L.; Sanchez, M.; Kouadio, Z.A.; Yao, A.B. Estimation de la sédimentation dans la retenue d'eau de la rivière Lobo à l'aide de la théorie des bassins de décantation. *XVIèmes Journées* **2020**, 249–258. [CrossRef]
13. Li, W.; Yang, S.; Hu, J.; Fu, X.; Zhang, P. Field measurements of settling velocities of fine sediments in Three Gorges Reservoir using ADV. *Int. J. Sediment Res.* **2016**, *31*, 237–243. [CrossRef]
14. Tian, C.; Zheng, S.; Su, M. An ultrasound-based monitoring of kaolinite flocculent settling processes. *Appl. Acoust.* **2023**, *203*, 109186. [CrossRef]
15. Sanchez, M. Settling velocity of the suspended sediment in three high-energy environments. *Ocean. Eng.* **2006**, *33*, 665–678. [CrossRef]
16. Krone, R.B. The Significance of Aggregate Properties to Transport Processes. In *Estuarine Cohesive Sediment Dynamics*; Mehta, A.J., Ed.; Springer: New York, NY, USA, 1986; pp. 66–84. [CrossRef]
17. Tattersall, G.; Elliott, A.; Lynn, N. Suspended sediment concentrations in the Tamar estuary. *Estuar. Coast. Shelf Sci.* **2003**, *57*, 679–688. [CrossRef]
18. Avenard, J.M. *Aspects du Contact Foret-Savane dans le Centre et l'Ouest de la Cote d'Ivoire: Etude descriptive*; IRD Editions: Kowloon, Hong Kong, 1974; p. 35.
19. Yao, A.B.; Goula, T.A.; Kouadio, Z.A.; Kouakou, K.E.; Kane, A.; Sambo, S. Analyse de la variabilité climatique et quantification des Ressources en eau en zone tropicale humide: Cas du basin. Versant de la lobo au centre-ouest de la Côte d'Ivoire. *Rev. Ivoir. Des Sci. Technol.* **2012**, *19*, 136–157.
20. Koffi, B.; Kouadio, Z.A.; Kouassi, K.H.; Yao, A.B.; Sanchez, M.; Kouassi, K.L. Impact of Meteorological Drought on Streamflows in the Lobo River Catchment at Nibéhibé, Côte d'Ivoire. *JWARP* **2020**, *12*, 495–511. [CrossRef]
21. Maiga, A.H.; Denyigba, K.; Allorent, J. Eutrophisation des petites retenues d'eau en Afrique de l'Ouest: Causes et conséquences: Cas de la retenue d'eau sur la Lobo à Daloa en Côte d'Ivoire. *Sci. Technol.* **2001**, *7*, 16–29.
22. Avenard, J.M. *Aspect de la Géomorphologie*; Avenard, J.M., Eldin, M., Girard, G., Sircoulon, J., Touchebeuf, P., Guillaumet, J.L., Adjanohoun, E., Perraud, A., Eds.; Mémoire ORSTOM: Paris, France, 1971; p. 50.
23. Kouassı, K.L.; Kouame, K.I.; Konan, K.S.; Angulo, M.S.; Deme, M.; Meledje, N.H.E. Two-Dimensional Numerical Simulation of the Hydro-Sedimentary Phenomena in Lake Taabo, Côte d'Ivoire. *Water Resour. Manage.* **2013**, *27*, 4379–4394. [CrossRef]
24. Lowrance. *ELITE Ti, Manuel de l'utilisateur*; Lowrance Electronics, Inc.: Tulsa, OK, USA, 2019.
25. Association française de normalisation (AFNOR). *Qualité de l'eau: Environnement, Sssociation Française de Normalization*, 1st ed.; AFNOR: Paris, France, 1994.
26. Sanchez, M. Effects of convective-diffusive vertical mixing on the conception of rectangular settling basins. *Stoch. Environ. Res. Risk Assess.* **2018**, *32*, 1457–1463. [CrossRef]
27. Huang, R.; Zhang, Q.; Zhang, W.; Li, Z. Experimental research on the effect of suspended sediment stratification on turbulence characteristics. *Estuar. Coast. Shelf Sci.* **2022**, *278*, 108128. [CrossRef]
28. Yan, H.; Kouyi, G.L.; Gonzalez-Merchan, C.; Becouze-Lareure, C.; Sebastian, C.; Barraud, S.; Bertrand-Krajewski, J.-L. Computational fluid dynamics modelling of flow and particulate contaminants sedimentation in an urban stormwater detention and settling basin. *Environ. Sci. Pollut. Res.* **2014**, *21*, 5347–5356. [CrossRef]
29. Khawaja, B.A. Evolutions morphologiques induites par l'implantation de barrages dans les fleuves à fort débit solide. Ph.D. Thesis, Université de Nantes, Nantes, France, 2011.
30. Dramais, G.; Camenen, B.; Le Coz, J. Comparaison de methodes pour la mesure des matieres en suspension dans les cours d'eau, en présence de sable. *La Houille Blanche* **2018**, *104*, 96–105. [CrossRef]

31. Endalew, L.; Mulu, A. Estimation of reservoir sedimentation using bathymetry survey at Shumburit earth dam, East Gojjam zone Amhara region, Ethiopia. *Heliyon* **2022**, *8*, e11819. [CrossRef]
32. Hountondji, B.; Codo, F.; Ahoumenou, Y.; Sintondji, L.O.; Ahouansou, L. Infiltration des eaux et des depots dans la retenue du mini-barrage de wourowourokou dans le nord du benin. *Larhyss J.* **2019**, *16*, 201–214.
33. Mélèdje, N.H. Modelisation de la Dynamique hydrologique Et du flux des sediments Dans le lac du barrage hydroelectrique d'Ayamé 1. Ph.D. Thesis, Université Nanguy Abrogoua, Abidjan, Côte d'Ivoire, 2015.
34. Achite, M.; Meddi, M. Spatial and temporal variability of streamflow and solid yields in semiarid areas. Case of the oued Mina basin (Northwest Algeria). *J. Water Sci.* **2005**, *18*, 37–56.
35. Bouguerra, S.-A.; Bouanani, A. Analyse saisonnière et interannuelle de la dynamique des flux en suspension dans le bassin versant de l'oued Boukiou (nord-ouest de l'Algérie). *Geomorphologie* **2019**, *25*, 2. [CrossRef]
36. Bouguerra, S.-A.; Bouanani, A. Simulation study on the flow behavior of wet particles in the power-law liquid-solid fluidized bed. *Powder Technol.* **2023**, *415*, 118117. [CrossRef]
37. El Mahi, A.; Meddi, M.; Bravard, J.P. Analyse du transport solide en suspension dans le bassin versant de l'Oued El Hammam (Algérie du Nord). *Hydrol. Sci. J.* **2012**, *57*, 642–1661. [CrossRef]
38. Meledje, N.; Kouassi, K.; N'Go, Y.; Kouassi, K.; Savane, I.; Aka, K. Caractérisation des apports sédimentaires et morphologie du lac du barrage hydroélectrique d'Ayame 1 (Sud-Est Côte d'Ivoire). *Int. J. Bio. Chem. Sci.* **2014**, *8*, 1290. [CrossRef]
39. Yang, Y.; Zheng, J.; Zhu, L.; Zhang, H.; Wang, J. Influence of the Three Gorges Dam on the transport and sorting of coarse and fine sediments downstream of the dam. *J. Hydrol.* **2022**, *615*, 128654. [CrossRef]
40. Kouassi, L.K. Hydrologie, Transport Solide et Modélisation de la Sédimentation dans les Lacs des Barrages Hydroélectriques de Côte d'Ivoire: Cas du Lac de Taabo. Ph.D. Thesis, Université Abobo-Adjamé, Daloa, Côte d'Ivoire, 2007.
41. Hosseinzadeh-Tabrizi, A.; Ghaeini-Hessaroeyeh, M. Modelling of dam failure-induced flows over movable beds considering turbulence effects. *Comput. Fluids* **2018**, *161*, 199–210. [CrossRef]
42. Khoshkonesh, A.; Daliri, M.; Riaz, K.; Dehrashid, F.A.; Bahmanpouri, F.; Di Francesco, S. Dam-break flow dynamics over a stepped channel with vegetation. *J. Hydrol.* **2022**, *613*, 128395. [CrossRef]
43. Schmidt, J.C. Effects of Dams on Rivers. In *Reference Module in Earth Systems and Environmental Sciences*; Elsevier: Amsterdam, The Netherlands, 2022; p. B9780128191668003000. [CrossRef]